

## ASSESSMENT OF PHOTOCATALYTIC CAPACITY OF A HYDRAULIC MORTAR

Pedro Castanho<sup>1</sup>, Vitor Silva<sup>1</sup> and Paulina Faria<sup>1,2\*</sup>

1: Dept. of Civil Engineering  
Universidade NOVA de Lisboa  
2829-516 Caparica, Portugal

e-mail: p.castanho@campus.fct.unl.pt, vmd.silva@fct.unl.pt, paulina.faria@fct.unl.pt

2: CERis – Civil Engineering Research and Innovation for Sustainability,  
Universidade de Lisboa,  
1049-001 Lisboa, Portugal

**Keywords:** Hydraulic lime, Mortar, Titanium dioxide, Self-cleaning

**Abstract:** *In urban areas façades of buildings and monuments accumulate dirt and are visually degraded, implicating high consumption of resources for repair. The search and development of new products that can help to maintain those façades is therefore very important.*

*To prevent possible damage to the building surface maintaining their aesthetic appearance, cementitious materials with new properties have been developed. One possibility arises from the introduction of titanium dioxide (TiO<sub>2</sub>) into the composition of coating materials. When exposed to solar UV radiation, the coatings lead to photo-induced oxidation of compounds adsorbed or deposited on their surfaces, with self-cleaning effect. This self-cleaning property reduces the need for maintenance. It can be an advantage for unpainted renders.*

*In this research, physic-mechanical characterization and evaluation of the self-cleaning capacity of a commercial hydraulic lime mortar with photocatalytic property, by the addition of TiO<sub>2</sub>, were carried out. Two mortars with 1:3 (binder:aggregate) volumetric proportion were produced, only differing on the aggregate type, namely its particle size distribution, and compared with similar mortars but formulated with a common hydraulic lime without TiO<sub>2</sub>. In the physic-mechanical characterization mortar specimens were laboratory tested for mechanical strength, open porosity, capillary water absorption and drying capacity. The self-cleaning capacity of mortars was evaluated by monitoring the discolouration of two organic dyes stains (Rhodamine B and Methylene Blue), applied on the surface of mortar specimens, when exposed to sunlight and UV light.*

*The mortars with TiO<sub>2</sub> shown improvements mainly in terms of mechanical strengths but without significant changes concerning water and vapour behaviour. Simultaneously those mortars have shown a great degradation of colour of the two dyes stains, with high colour change percentages particularly after sunlight exposure.*

## 1. INTRODUCTION

Currently, the preservation of the environment and the protection of architectural heritage, are issues of great awareness. As such, the demand for more sustainable and environmentally friendly materials has been increasing.

The application of photocatalysts like titanium dioxide ( $\text{TiO}_2$ ) to construction materials has been tested in many studies, which report the self-cleaning effect of mortars and cement pastes [1, 2, 3, 4, 5]. Maury-Ramirez et al. [4] noted that adding  $\text{TiO}_2$  to coatings can be more effective because the coatings are in direct contact to photons and pollutants. The  $\text{TiO}_2$  exposed to solar UV rays can actively participate in photocatalysis leading to oxidation of compounds adsorbed or deposited on surfaces of coatings.

The photocatalytic ability is typically defined in terms of dyes degradation efficiency and can be assessed according an Italian standard (UNI 11259 [6]). In order to verify self-cleaning performances of photocatalytic construction materials, several tests involving organic substances degradation on surfaces of materials formulated with  $\text{TiO}_2$  have been set up and include the degradation of colour in dyes, such as Rhodamine B and Methylene Blue [2, 3, 4] under different exposure conditions. Results have shown efficient degradation of the dyes colour under both UV light and visible light.

In this study a commercial hydraulic lime with addition of  $\text{TiO}_2$  (and most probably other additions) was used. The aim of this lime with hydraulic properties is to associate photocatalytic properties with characteristics that are supposed to be compatible with old masonry supports and, at the same time, present good durability. That would makes it very beneficial when applied on the rehabilitation of building renders or for rendering unpainted new buildings.

In the study the ability of mortars with this hydraulic lime with photocatalytic property to self-clean organic dyes made on the surface of rendering samples under UV and natural sunlight is assessed in comparison with a common natural hydraulic lime. The influence of the use of sands with different particle size distribution is also evaluated. Physic-mechanical characterization is reported to assess the changes on mortars with this new lime with hydraulic properties and  $\text{TiO}_2$  addition.

## 2. MATERIALS AND METHODS

### 2.1. Materials, mortars and samples

A hydraulic lime with  $\text{TiO}_2$  (among other unknown admixtures), commercialized as Cal TI HL5 by SECIL Argamassas, was used (designated as TI in this text). Based on the producers oral information, the lime has more than 4% of  $\text{Ca}(\text{OH})_2$  and less than 3% of sulphates. A common hydraulic lime, commercialized as Martigança HL5, was also used as reference (HL5). Both limes are classified by EN 459-1 [7]. Two different types of sands were used as aggregate: a coarser particle size sand from Sesimbra, Portugal (S), and a mixture of four types of sand with different particle sizes (M), which particle size distributions can be observed in Figure 1. The loose bulk density of the four materials is presented in Table1.

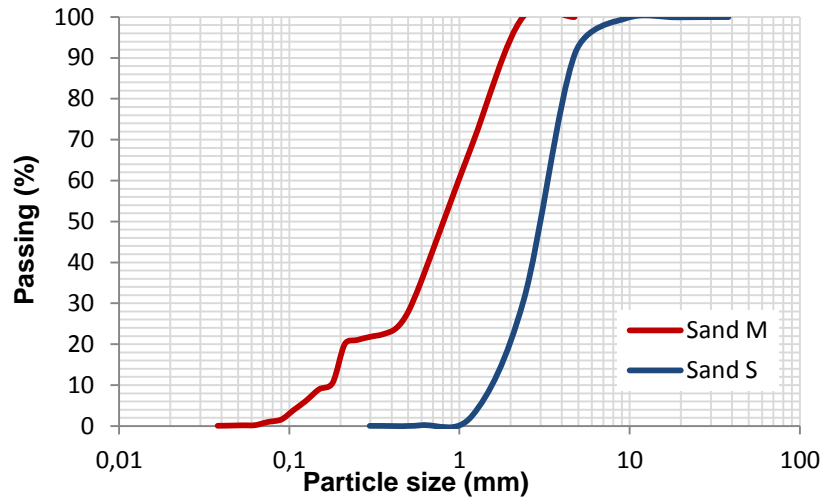


Figure 1. Particle size distribution of the sands

Table 1. Loose bulk density of the binders and sands

Material	TI HL5	HL5	Sand S	Sand M
Loose bulk density (g/cm <sup>3</sup> )	0.756	0.748	4.414	4.873

Four mortars were formulated with both limes and mortars: two ordinary mortars (SHL5 and MHL5) and two photocatalytic mortars (STI and MTI). The mass and volumetric proportions of mortars are presented in table 2.

Table 2. Mass and volumetric proportions, water/binder ratio and flow table consistency of mortars

Mortar	Mass proportion (binder:sand)	Volumetric proportion (binder:sand)	Water/binder (-)	Flow value (mm)
SHL5	1:5.9	1:3	1.5	172
STI	1:5.8		1.5	171
MHL5	1:6.5		1.2	172
MTI	1:6.4		1.2	170

The mixing procedure was carried out based on EN 1015-2 [8]. The water was added to achieve a flow table consistency of  $170 \pm 2$  mm, based on EN 1015-3 [9]. Water/binder ratio (by weight) and the flow table consistency of mortars are presented in Table 2. Mortars were cast in two types of moulds with dimensions  $40 \times 40 \times 160$  [mm] and  $100 \times 100 \times 30$  [mm] and cured for 28 days at  $20 \pm 2^\circ\text{C}$  and  $65 \pm 5\%$  relative humidity.

## 2.2. Physic-mechanical characterization

Flexural and compressive strengths of mortars were determined according to EN 1015-11 [10]. One half of each prismatic specimens with  $40 \times 40 \times 160$  [mm] after the flexural strength test was used for the compressive strength test, that result other portion used for the determination of open porosity that was determinate following based on EN 1936 [11].

Capillary water absorption and drying capacity were assessed based on EN 15801 [12] and EN 16322 [13], respectively. The other half of each prismatic sample was cut down to specimen with 60 mm height. The lateral faces were waterproofed with hot wax. For capillary the samples were weighted when dried and after defined periods of time of contact with 5mm of water. When saturated by capillary, they were removed from the contact with water and weighted again after defined periods of drying.

### 2.3. Self-cleaning performance

Self-cleaning capability of photocatalytic mortars was determined by monitoring the discoloration of two organic dyes: Rhodamine B (RhB) and Methylene Blue (MB). Experiments were carried out for both dyes based on the procedure described in UNI 11259 [6], with some modifications: using the 100×100×30 [mm] samples and 0.1 g/l concentration of RhB solution. Based on the Italian standard [6], the MB was applied with 0.05 g/l and for both dyes 0.5 ml of each were applied.

The specimens were exposed to sunlight for 586h, for an average period of 12h per day of direct sun exposure, and to UV light all day for 1176h total.

Colour measurements were taken directly on the surface of each specimen at different times under sunlight and UV light, with a portable colorimeter Datacolor, Microflash 4.0. The results were expressed in the CIELAB system [1, 5] with **L**, **a** and **b** colourimetric coordinates (**a** for red/green and **b** for yellow/blue). The percentage of colour change was expressed with the coordinate of dominant colour of dye **a** (red) or **b** (blue) for RhB and MB, respectively, according to equations 1 and 2.

$$\text{Colour change} = \frac{a_0 - a_t}{a_0} \cdot 100 [\%] \quad (1)$$

$$\text{Colour change} = \frac{b_0 - b_t}{b_0} \cdot 100 [\%] \quad (2)$$

where **a**<sub>0</sub> and **b**<sub>0</sub> are the colour intensity coordinates of specimens before the light exposure, **a**<sub>t</sub> and **b**<sub>t</sub> are the colour intensity coordinates of specimens after t hours of exposure.

## 3. RESULTS AND DISCUSSION

### 3.1. Effect on physic-mechanical mortar properties

Table 3 presents the mechanical strengths and open porosity of the mortars. The mortars with lime with TiO<sub>2</sub> nanoparticles show an improvement in both flexural and compressive strength with both sands. The two photocatalytic mortars reached higher values, compared to mortars with common hydraulic lime without TiO<sub>2</sub>, probably due to the presence of nanoparticles that could play a filler effect or to the combined effect of other admixtures included in the TI formulation. The biggest increase was observed in mortars with M sand (sand with finer particle size), MTI, with compressive strength almost doubling its value. The higher the porosity, the lower the flexural and compressive strengths of the materials, as expected.

However the open porosity, with the incorporation of  $\text{TiO}_2$ , does not change too much, decreasing only 1% in MTI specimen and no effect was observed in STI.

Table 3. Flexural and compressive strengths and open porosity of mortars

Mortar	Flexural strength (MPa)		Compressive strength (MPa)		Porosity (%)	
	Average	StDv	Average	StDv	Average	StDv
SHL5	0.30	0.04	2.72	0.16	26.0	0.2
STI	0.32	0.02	3.31	0.04	26.2	0.7
MHL5	0.43	0.05	4.72	0.17	23.0	0.3
MTI	0.58	0.04	7.46	0.25	22.4	0.5

Results of capillary water absorption can be observed in the capillary curves of mortars presented on Figure 2.

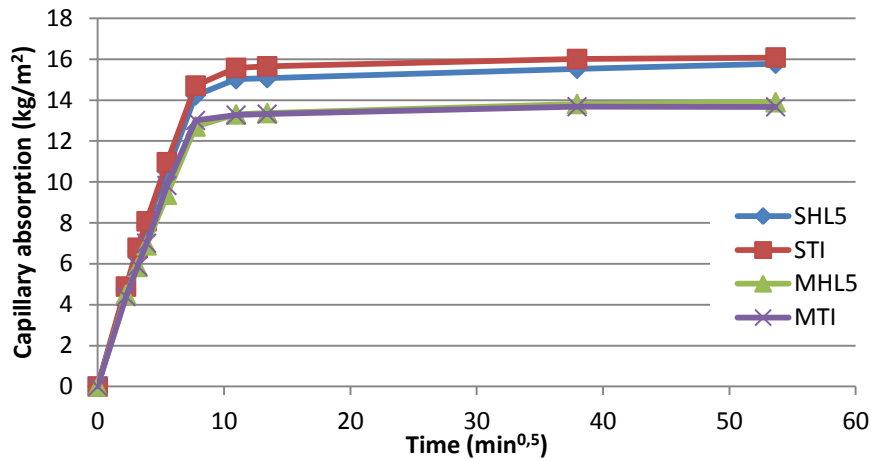


Figure 2. Capillary curve of mortars

The slope of the initial linear segment of the capillary curve represents the capillary coefficient of mortars (CC), showing the speed of capillary water absorption, while the asymptotic value (AV) represents the total amount of water that can be absorbed by capillarity. Results of capillary coefficient and asymptotic value are presented in Table 4.

Table 4. Capillary coefficient, asymptotic capillary value, drying rate and drying index of mortars

Mortar	CC [ $\text{kg/m}^2 \cdot \text{min}^{0.5}$ ]		AV ( $\text{kg/m}^2$ )		DR [ $\text{kg/m}^2 \cdot \text{h}$ ]		DI (-)	
	Average	StDv	Average	StDv	Average	StDv	Average	StDv
SHL5	1.70	0.05	15.8	0.01	0.16	0.01	0.19	0.01
STI	1.77	0.04	16.1	0.20	0.16	0.01	0.20	0.00
MHL5	1.50	0.02	13.9	0.14	0.15	0.00	0.19	0.00
MTI	1.58	0.03	13.7	0.05	0.14	0.00	0.20	0.01

Results of drying can be observed in the drying curves of mortars, in function of time, presented in Figure 3. This curves allow to visualize the first phase of drying; similar curves but in function of the square root of time would allow to visualize the second phase of drying.

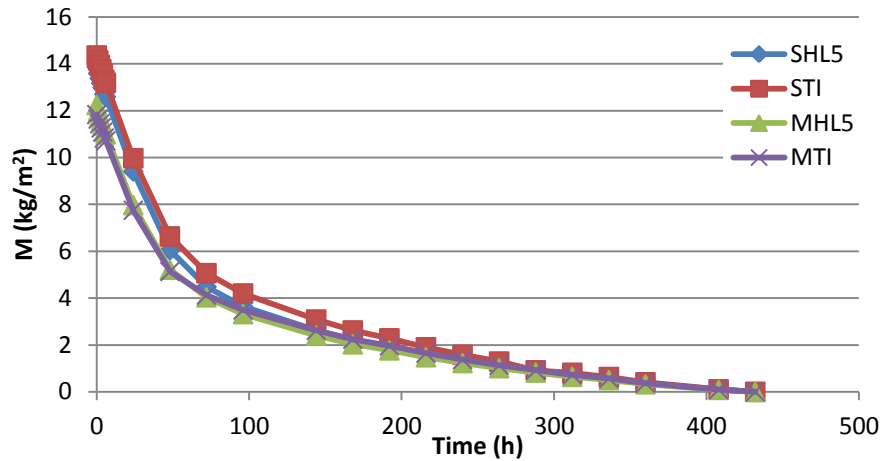


Figure 3. Drying curve of mortars, in function of time

The slope of the initial linear segment of the curves represent the 1<sup>st</sup> phase drying rate of mortars (DR), that expresses the speed of initial drying, while the whole graph allows to determine the drying index (DI), which expresses the resistance to complete drying. Results are presented in Table 4.

As can be observed in Table 4, the STI mortar presents the highest CC and DR. This means that the mortar has a fast capillary absorption but can also release it quickly. In the other hand, MHL5 mortar absorbs water much slowly but loses it much slowly in the drying process. Mortars with finer particle size aggregate (M) present lower CC, which increases with the addition of TiO<sub>2</sub>. The drying rates are very similar for mortars with each type of sand, although they decreased with the incorporation of TiO<sub>2</sub> nanoparticles in MTI mortar. The drying process is faster for mortars with finer sand S in comparison with M sand mortars. Nevertheless, concerning CC and DR the influence of the type of sand is much stronger than the type of lime.

Also in the same Table 4, it can be seen that the mortar with the lower AV, is the same with the higher DI, which means that this mortar (MTI) absorbs less quantity of water but has more difficulty in releasing it. This can be explained to the fact that MTI shows the lowest open porosity. Another finding that can be seen is that the mortars with TiO<sub>2</sub> present relatively higher drying index, in comparison with the similar mortars without TiO<sub>2</sub>, indicating a lower total drying capacity of TI mortars. The mortars with finer sand M present the lowest AV, what is positive for the water behavior. Although in terms of AV the influence of the type of sand is stronger than the type of lime, concerning DI the inverse situation occurs, being the influence of the type of lime more important.

### 3.2. Photocatalytic efficiency

Decomposition of the Rhodamine B and Methylene Blue dyes has been tried for all the mortar formulations according to the procedure previously described. In order to see more results of the self-cleaning performance, colour changes before and after 4h and 26h (the observation periods of time defined in the standard UNI 11259 [6]) of both light irradiations are reported.

The self-cleaning activity of  $\text{TiO}_2$  hydraulic lime and reference mortar surfaces, represented by the degradation evolution of RhB and MB stains, is given in Tables 5 and 6, showing a quick look up on dye photo degradation after a longer exposure time. It can be observed that under exposure, the colour reduces as a function of time, i.e. the dye molecule degrades. All mortars with  $\text{TiO}_2$  were able to degrade completely RhB under both light exposures. For the MB degradation, the mortars under sunlight exposure showed better results.

Table 5. Stains on mortars at 0h and 586h after sunlight exposure






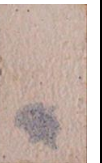


















0h				586h			
SHL5	STI	MHL5	MTI	SHL5	STI	MHL5	MTI
							
							
							

Table 6. Stains on mortars at 0h and 1176h after UV light exposure

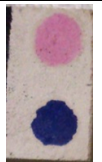




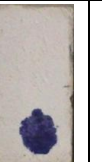
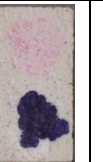


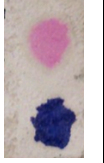

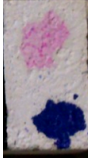

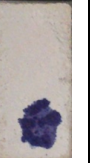



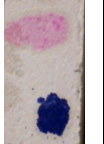



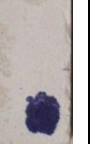
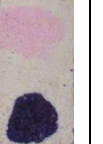

0h				1176h			
SHL5	STI	MHL5	MTI	SHL5	STI	MHL5	MTI
							
							
							

Figure 4 shows the percentages of colour change for RhB stain on mortars after exposure to daylight. Generally, the results indicate that the photocatalytic mortars performed better than the mortars without  $\text{TiO}_2$ . It can be observed a very high initial reaction rate, with values quite

similar between STI and MTI. The difference between mortars is less significant after 26h. Overall all four hydraulic lime mortars showed a very high percentage of colour change: above 90%.

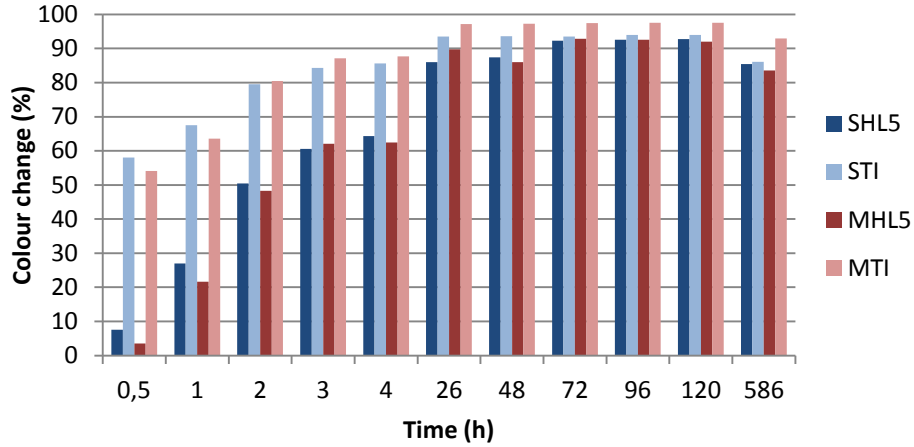


Figure 4. Colour change of RhB stain on mortars after sunlight exposure

The degradation rate of colour of RhB under UV irradiation can be seen in Figure 5. The results indicate that photocatalysis was mostly effective after the first 26h of illumination. Nevertheless, high colour change percentage was achieved only by mortars with  $\text{TiO}_2$  as expected. Both mortars, STI and MTI, had similar results over time.

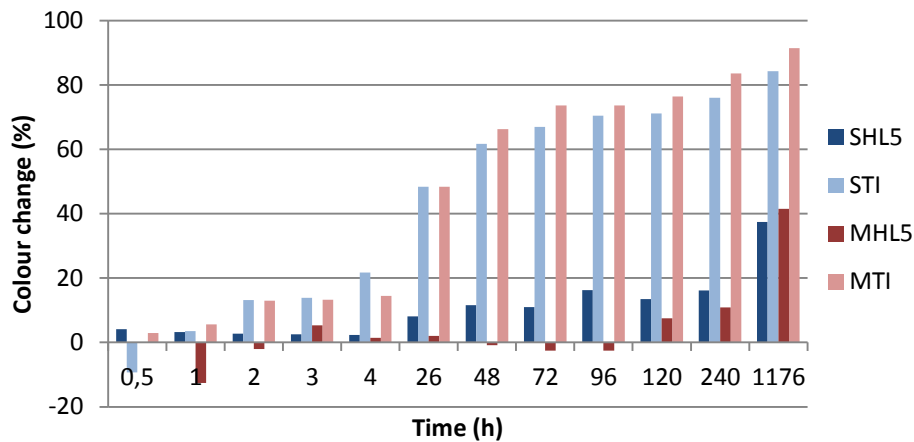


Figure 5. Colour change of RhB stain on mortars after UV light exposure

Methylene Blue stains showed a slight different result in their degradation. From the results in Figure 6, it can be observed that for sunlight exposure the values for all four mortars are quite similar. It can be noted that there is also degradation of colour in mortars which do not contain  $\text{TiO}_2$ . However, even by taking account of this effect, it can be shown that there is an enhanced degradation of colour in the presence of photocatalyst, showing a self-cleaning effect.



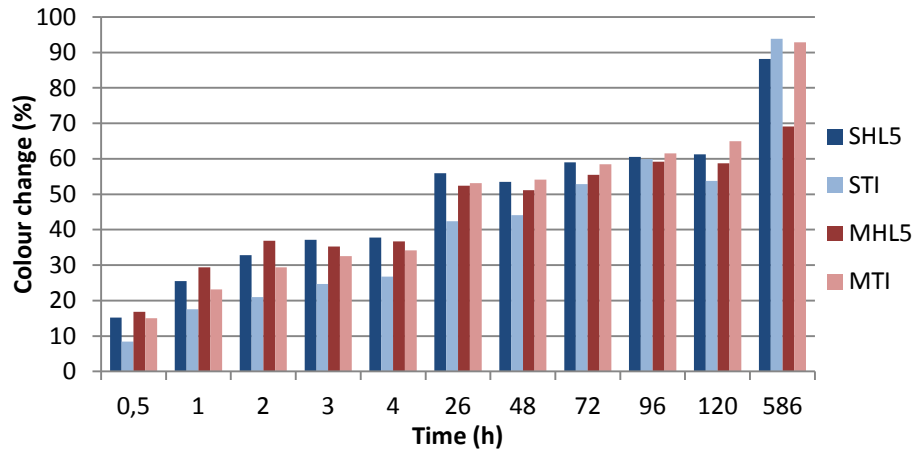


Figure 6. Colour change of MB stain on mortars after sunlight exposure

Figure 7 shows the colour change of MB stain on mortars after UV light exposure. The lower energy available from UV light seems to be insufficient to induce photodegradation of MB not allowing to high percentage values of colour change. The two mortars without  $\text{TiO}_2$  showed higher percentages of colour change in comparison with the photocatalytic mortars, although with values not over 50%.

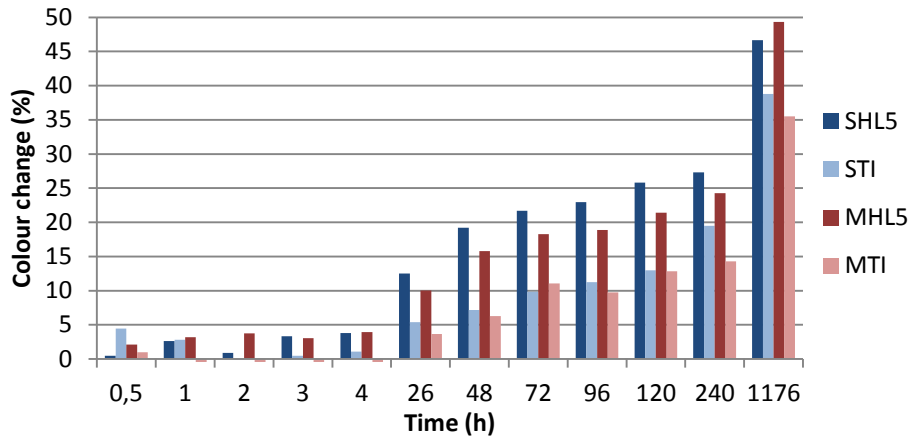


Figure 7. Colour change of MB stain on mortars after UV light exposure

#### 4. CONCLUSIONS

Based on the results and discussion, it is possible to conclude that the incorporation of  $\text{TiO}_2$  nanoparticles affected the physical characteristics of the mortars, as exemplified by the improvements in mechanical strengths, mostly in the mortars with finer particle size aggregate, MTI. Mortars with  $\text{TiO}_2$  does not showed to greatly change the behavior presented by the HL5 reference mortars, with similar results of capillary water absorption and drying capacity.

$\text{TiO}_2$  mortars with both types of sands show high potential towards discoloration of RhB and MB stains with removal efficiencies higher than 90% under sunlight. After UV light

exposure, the same mortars had good results in colour change of RhB with higher percentage for the mortar MTI. Nevertheless, the MB stain in TiO<sub>2</sub> mortars under UV light showed low colour change in the period of time of test.

## REFERENCES

- [1] E. Relinque, J. Garcia, A. Castillo, M. Castellote, “Characteristics and efficiency of photocatalytic cementitious materials: Type of binder, roughness and microstructure”. *Cement and Concrete Research*, vol. 71, pp. 124–131, 2015.
- [2] C. Mendoza, A. Valle, M. Castellote, A. Bahamonde, M. Faraldos, “TiO<sub>2</sub> and TiO<sub>2</sub>–SiO<sub>2</sub> coated cement: Comparison of mechanic and photocatalytic properties”. *Applied Catalysis B: Environmental*, vol. 178, pp. 155–164, 2014.
- [3] P. Krishnan, M. Zhang, L. Yu, H. Feng, “Photocatalytic degradation of particulate pollutants and self-cleaning performance of TiO<sub>2</sub>-containing silicate coating and mortar”. *Construction and Building Materials*, vol. 44, pp. 309–316, 2013.
- [4] A. Maury-Ramirez, K. Demeestere, N. Belie, “Photocatalytic activity of titanium dioxide nanoparticle coatings applied on autoclaved aerated concrete: effect of weathering on coating physical characteristics and gaseous toluene removal”. *Journal of Hazardous Materials*, vol. 211-212, pp. 218–25, 2012.
- [5] B. Ruot, A. Plassais, F. Olive, L. Guillot, L. Bonafous, “TiO<sub>2</sub>-containing cement pastes and mortars: Measurements of the photocatalytic efficiency using a rhodamine B-based colourimetric test”. *Solar Energy*, vol. 83, pp. 1794–1801, 2009.
- [6] UNI 11259:2008 - Determinazione dell'attività fotocatalitica di leganti idraulici - Metodo della Rodamina B.
- [7] EN 459-1:2010 – Building lime. Definitions, specifications and conformity criteria.
- [8] EN 1015-2:1998/A1:2006 - Methods of test for mortar for masonry. Part 2: Bulk sampling of mortars and preparation of test mortars.
- [9] EN 1015-3:1999/A1:2004/A2:2006 – Methods of test for mortar for masonry. Part 3: Determination of consistence of fresh mortar (by flow table).
- [10] EN 1015-11:1999/A1:2006 - Methods of test for mortar for masonry. Part 11: Determination of flexural and compressive strength of hardened mortar.
- [11] EN 1936:2006 – Natural stone test methods. Determination of real density and apparent density, and of total and open porosity.
- [12] EN 15801:2009 – Conservation of cultural property. Test methods. Determination of water absorption by capillarity.
- [13] EN 16322:2013 – Conservation of cultural heritage. Test methods. Determination of drying properties.